Photochemistry of the Furan-Side 8-Methoxypsoralen–Thymidine Monoadduct Inside the DNA Helix. Conversion to Diadduct and to Pyrone-Side Monoadduct†

John W. Tessman, Stephen T. Isaacs, and John E. Hearst*
Department of Chemistry, University of California, Berkeley, California 94720
Received July 23, 1984

ABSTRACT: We have studied the photochemical reactions of 8-methoxypsoralen (8-MOP) with calf thymus DNA. Analysis of the photoproducts formed was carried out by enzymatic digestion of the 8-MOP-modified DNA, followed by HPLC separation of photoadducts by high-pressure liquid chromatography (HPLC). The 4′,5′ (furan-side) monoadduct of 8-MOP bound to thymidine is converted to cross-linked thymidine–8-MOP–thymidine diadduct by 341.5 nm light with a quantum yield of 0.028 ± 0.004. This is 4 times greater than the quantum yield for initial adduct formation (0.0065 ± 0.0004). When low levels of 8-MOP are covalently bound to DNA by using 397.9 nm light, less than 10% of the adducts formed are diadducts yet nearly 70% are in 5′-TpA cross-linkable sites. The furan-side monoadducts in these sites can subsequently be converted to diadduct or to a lesser extent 3,4 (pyrone-side) monoadduct.

Psoralens are a class of compounds that have been used as photosensitizing agents in the treatment of psoriasis and as probes in the elucidation of nucleic acid structure and function (Song & Tapley, 1979; Thompson & Hearst, 1983a,b). This usefulness of psoralens is the result of their photoreactivity with pyrimidine bases in nucleic acids. Psoralens intercalate between base pairs in the DNA double helix and form cycloaddition products with pyrimidine bases upon irradiation with long wavelength ultraviolet light. This cycloaddition can occur between the 5,6 double bond of a pyrimidine base and the 3,4 (pyrone) or 4′,5′ (furan) double bond of the psoralen (Straub et al., 1981; Kanne et al., 1982a). It is also possible to form interstrand cross-links via cycloaddition at both ends of a psoralen molecule (Kanne et al., 1982b). The structures of 8-methoxypsoralen (8-MOP), of the monoaddition products of 8-MOP and thymidine (dT) at the furan and pyrone side, and of the dT–8-MOP-dT diadduct, or cross-linked product, are shown in Figure 1. The reaction between 8-MOP and calf thymus DNA occurs almost exclusively with thymidine. While a small amount of reaction with cytosine does occur, in this report we consider only those sites in the DNA containing thymidine as reactive sites.

This study is primarily concerned with the quantification of the formation of the interstrand diadduct shown in structure **4** from the furan-side monoadduct shown in structure **2**. 8-Methoxypsoralen was selected as the psoralen derivative to be studied for three reasons. First, 8-MOP is probably the most widely used psoralen derivative for both research and clinical application. Second, the photochemical binding of 8-MOP to DNA results in the formation of a significant proportion of pyrone-side monoadduct (ca. 20%), which is not the case with all psoralen derivatives (Kanne et al., 1984). Finally, previous work has established procedures for the isolation and quantitative analysis of the various adducts formed between 8-MOP and DNA (Kanne et al., 1982b). Using these procedures, we have analyzed the adduct population under conditions where mostly monoadducts are formed and then monitored the conversion of these monoadducts to diadducts as a function of energy absorbed. In the course of the study, an interesting observation on the source of the pyrone-side monoadduct has been made.

Our results show that (1) the quantum yield for conversion of furan-side monoadduct to diadduct is approximately 4 times greater than the quantum yield for initial photoaddition of 8-MOP to DNA, (2) furan-side monoadduct is converted not only to diadduct but also to pyrone-side monoadduct, and (3) at low levels of 8-MOP covalently bound to DNA, 8-MOP exhibits a preference for monoaddition at 5′-TpA cross-linkable sites. While our observations are consistent with a mechanism whereby furan-side monoadduct undergoes in-helix photoisomerization to form pyrone-side monoadduct, this mechanism must still be experimentally verified. We are currently addressing this problem.

Experimental Procedures

Materials. 8-([$^3H_3$]Methoxy)psoralen was obtained from HRI Associates, Inc. (Emeryville, CA). Calf thymus DNA and all hydrolytic enzymes were obtained from Sigma Chemical Co. (St. Louis, MO).

Dark Binding. The dissociation constant was determined for the intercalation of 8-MOP into DNA by using equilibrium dialysis (Isaacs et al., 1977). Spectrapor 2 (Spectrum Medical Industries, Los Angeles, CA) dialysis tubing was boiled in a saturated sodium bicarbonate solution for ca. 20 min. A 1-mL solution of 730 μg/mL DNA in 10 mM tris(hydroxymethyl)aminomethane (Tris)[1] /1 mM EDTA, pH 7.5, was tied in a dialysis bag and placed in 18 mL of ca. 30 μg/mL 8-MOP solution in 10 mM Tris/1 mM EDTA. This was allowed to equilibrate in the dark with stirring for 72 h. 8-MOP concentrations inside and outside of the dialysis bag were determined by scintillation counting, and the DNA concentration inside the bag was determined by measuring the optical density

†This work was supported by the National Institute of General Medical Sciences, Department of Health and Human Services, Grants GM25151 and GM11180. The Nd:YAG laser used in this study was purchased with NSF Grant CHE 8116042.

[1] Abbreviations: Tris, tris(hydroxymethyl)aminomethane; EDTA, ethylenediaminetetraacetic acid; HPLC, high-pressure liquid chromatography.

0006-2960/85/0424-1669$01.50/0

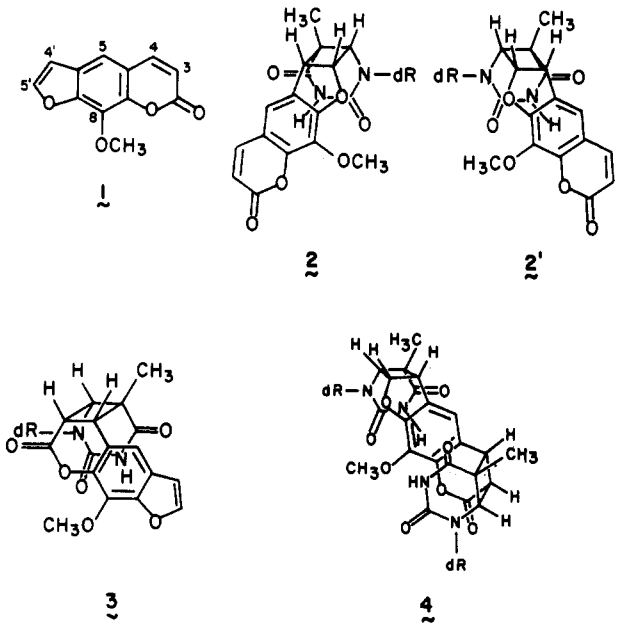

FIGURE 1: Structure of 8-methoxypsoralen (**1**), the two diastereomeric furan-side 8-MOP–dT monoadducts (**2**, **2'**), the pyrone-side 8-MOP–dT monoadduct (**3**), and the dT–8-MOP–dT diadduct (**4**).

at 258 nm (corrected for the absorbance of 8-MOP present with the DNA). The dissociation constant is expressed as K_D = [P][S]/[PS] where [P] = free 8-MOP concentration, [S] = concentration of free base pairs, and [PS] = concentration of 8-MOP intercalated into the DNA. This constant was used to determine the number of moles of 8-MOP intercalated inside the DNA helix, which is needed to calculate the quantum yield for initial adduct formation.

Photobinding. A schematic diagram of the irradiation apparatus is shown in Figure 2. Samples were irradiated by using a Quanta-Ray Model DCR-2A neodymium:YAG laser. This yielded 1064-nm pulses of 10 ns at 10 Hz. A harmonic generator converted this output to a 4th harmonic at 266 nm. This pulse has a duration of about 5 ns. The 4th harmonic was Raman shifted by using H_2 to give the desired wavelengths. The second and third Stokes lines of the 4th harmonic gave pulses of 341.5 and 397.9 nm, respectively. The energy absorbed by the samples was determined by monitoring the laser pulses with a calorimeter in line with a power meter and chart recorder as shown in Figure 2. Energy absorbed by a sample was determined as a difference between the power reading without sample and the reading when the sample was in the laser beam. The power meter reading was standardized by using uranyl oxalate actinometry (Weissberger, 1956). The major source of error in calculating the absorbed energy was due to fluctuations in the chart recorder trace of the power meter. We have estimated the experimental errors in the quantum yields based upon the fluctuations in these measurements. Although the beams were well separated, the 341.5- and 397.9-nm beams were also filtered with Turner long-pass filters so that no stray lower wavelengths would reach the sample. A 305-nm filter was used with the 341.5-nm line while both 345- and 360-nm filters were used with the 397.9-nm line. The quartz irradiation cell held 3-mL samples with a 1-cm path length and 2-cm diameter. A magnetic stirrer was required to keep the sample well distributed since the laser beam was generally less than 1 cm in diameter.

For the quantum yield determination of initial adduct formation at 341.5 nm, 8-[$^3H_3$]methoxypsoralen in ethanol (ca. 2.7 mg/mL) was added to a 730 μg/mL solution of calf thymus DNA in 10 mM Tris/1 mM EDTA (pH 7.5) buffer to give a solution which was 26 μg/mL in 8-MOP and 730 μg/mL in DNA. This solution was irradiated for various times at 341.5 nm (3 mL per irradiation). These irradiated samples were then extracted 4 times with 3 mL of chloroform, made 0.2 M in NaCl, and precipitated with 6 mL of 100% ethanol. The samples were cooled in dry ice/ethanol for 0.5 h and then centrifuged at 7000 rpm for 20 min. The DNA pellets were dried, redissolved in water, and then reprecipitated. These pellets were again dried and redissolved in water. These solutions were counted, and their optical density was measured at 258 nm on a Cary 118 spectrophotometer to determine the 8-MOP:DNA base pair photobinding ratio. The average molecular weight of a DNA base pair was taken to be 660 for the calculation. Quantum yields were determined by calculating the moles of 8-MOP covalently bound divided by the moles of photons absorbed by the intercalated 8-MOP.

For the quantum yield determination of conversion of furan-side monoadduct to dT–8-MOP–dT diadduct, a 30-mL sample of [^{3}H]-8-MOP/DNA was irradiated in a 10-cm path length, 2-cm diameter quartz cell, at 397.9 nm to a total binding of ca. 100 base pairs per 8-MOP. This solution was extracted 4 times with 30 mL of chloroform and precipitated twice with NaCl/ethanol as described earlier. The final pellet was redissolved in 10 mM Tris/1mM EDTA (pH 7.5) buffer to a DNA concentration of ca. 750 μg/ml. A 3-mL sample of this was reprecipitated and redissolved in 15 mM sodium

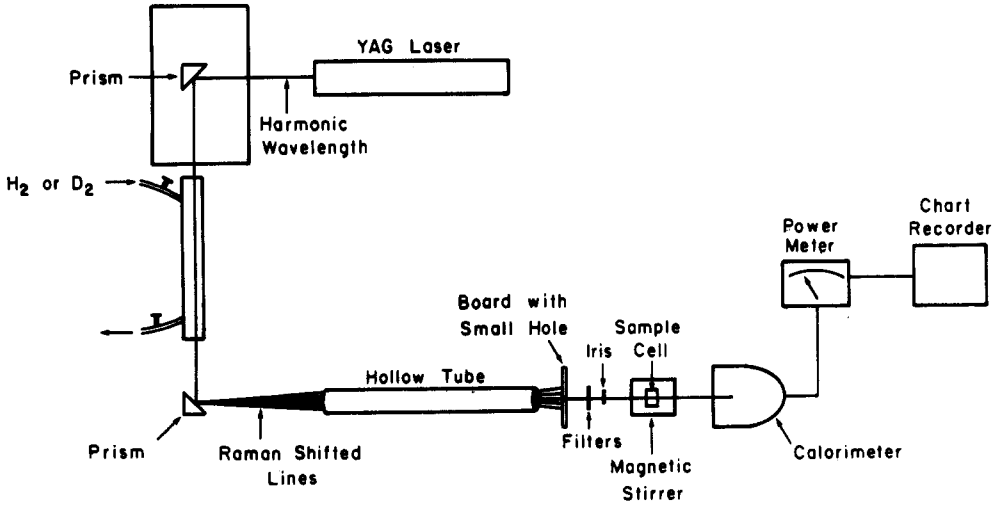

FIGURE 2: Schematic diagram of the laser irradiation apparatus.

acetate (pH 5) buffer for enzymatic hydrolysis. Samples of 3 mL of the 397.9-nm 8-MOP/DNA stock were then irradiated for various times at 341.5 nm. These samples were also precipitated and redissolved in sodium acetate for hydrolysis. This hydrolysis was done by adding 80 units of DNase II (EC 3.1.4.6) per mg of DNA in the sodium acetate buffer. This solution was placed in a 37 °C water bath for 12 h at which time another 80 units/mg of DNA of DNase II was added. After an additional 12 h at 37 °C, the solution was adjusted to pH 7 with Tris base, and 0.2 unit/mg of DNA of phosphodiesterase II (EC 3.1.4.18) was added. This was returned to 37 °C for 24 h before another dose of phosphodiesterase II was added. After another 24 h at 37 °C, the solution was adjusted to pH 8 and 0.2 unit of bacterial alkaline phosphatase (EC 3.1.3.1) per mg of DNA was added. This was placed at 37 °C for 24 h. The digested solution was prepared for HPLC by adjusting to ca. pH 3 with phosphoric acid and centrifuging to give a clear supernatant. Scintillation counting of the solution before and after centrifugation established that no tritium counts cosedimented with the pellet. This supernatant was then injected on an Altex/Beckman reverse-phase C18 ODS HPLC column with 10 mM KH_2PO_4 (pH 2.2) buffer and methanol as the eluting solvents. Eighty fractions were collected, with the absorbance being monitored at 250 nm. The fractions were assayed for tritium by scintillation counting. The fractions were identified by their retention times and their ultraviolet absorption spectra which were entirely consistent with their assignment to dT–8-MOP–dT diadduct, dT–8-MOP furan-side monoadduct, and dT–8-MOP pyrone-side monoadduct as reported elsewhere (Kanne et al., 1982a,b). The solvent gradient was as follows: 0–10 min, 100% buffer; 10–25 min, 100–70% buffer; 25–45 min, 70% buffer; 45–75 min, 70–0% buffer. This gradient was altered slightly from the reported procedure to allow for a better separation of the various adducts. The quantum yield for conversion of furan-side monoadduct to diadduct was determined by dividing the moles of cross-link appearing by the moles of photons absorbed by the portion of the furan monoadduct competent to form cross-link. Quantum yields were calculated for the initial linear region of the plot of percent diadduct vs. energy absorbed.

Conversion of Furan-Side Monoadduct to Pyrone-Side Monoadduct. An irradiation device (Isaacs et al., 1977) giving a 320–380-nm band of light was used to further investigate the possibility of photoisomerization of furan-side monoadduct to pyrone-side monoadduct. The irradiation device consisted of two 400-W General Electric mercury vapor lamps with a cobaltous nitrate filter (40% w/w). First a sample of [^{3}H]-8-MOP/DNA was prepared by irradiating at 397.9 nm, and a portion of the sample was analyzed as described above to establish the adduct distribution. The remainder of the sample was dissolved in 10 mM Tris/1 mM EDTA (pH 7.5) buffer to a final DNA concentration of 630 μg/mL. From this solution, 3-mL samples were removed and reirradiated with either the Nd:YAG laser at 341.5 nm or the 320–380-nm irradiation device. Irradiations were carried out with more than twice the energy absorbed by the final time point of Figure 5 (see Table III). These samples were precipitated, dried, and analyzed to determine the adduct distribution as described above.

The 320–380-nm irradiation device was also used to look at the stability of 8-MOP bound to DNA with respect to photoreversal upon extended irradiation. A 2-mL sample of [^{3}H]-8-MOP plus DNA in 10 mM Tris/1 mM EDTA (pH 7.5) was irradiated for 10 min with the irradiation device. This sample was extracted 4 times with 2 mL of chloroform and the DNA precipitated as described above. The pellet was redissolved in 2 mL of 10 mM Tris/1 mM EDTA, pH 7.5, and irradiated on the 320–380-nm irradiation device. Aliquots of 100 μL were removed at 1, 5, 10, 30, and 60 min, extracted as before with chloroform, and precipitated. These samples were redissolved in 1.5 mL of H_2O, and the binding ratio was determined by taking the UV absorbance at 258 nm and by ^{3}H scintillation counting.

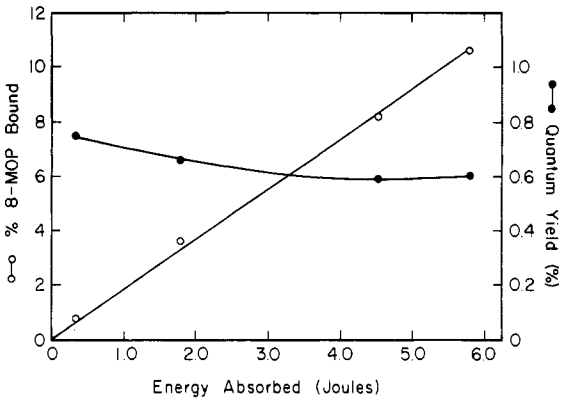

FIGURE 3: Irradiation of an 8-MOP/DNA solution at 341.5 nm with the YAG laser. The percent psoralen bound (○) is shown as a function of energy absorbed. The quantum yield (●) is also indicated for each irradiation point.

RESULTS

Dark Binding of 8-MOP to DNA. Equilibrium dialysis experiments were performed to determine the number of 8-MOP molecules bound to the DNA prior to irradiation. The extent of the dark binding is expressed by the dissociation constant K_D. The dissociation constant was determined to be 1.8×10^{-3} mol/L at the DNA and 8-MOP concentrations used in the quantum yield experiments. This number was used to calculate the amount of psoralen noncovalently bound to the DNA, which in turn was used in the calculation for normalization of the total number of photons absorbed by the sample to only those absorbed by 8-MOP molecules actually intercalated within the DNA helix.

Quantum Yield of Adduct Formation between 8-MOP and DNA. Noncovalently bound 8-MOP undergoes photocycloaddition to give covalent monoadduct in the photoaddition step. At the beginning of the photoreaction, the formation of covalent adduct is linear with time. To determine the quantum yield, the number of adducts formed at each linear time point was divided by the number of photons absorbed by the intercalated 8-MOP molecules. Implicit in the calculation of each point is the assumption that no significant change in the amount of intercalated 8-MOP occurred.

Figure 3 shows four linear time points of an 8-MOP/DNA solution irradiated at 341.5 nm with the YAG laser. During this period the formation of adduct is a first-order process, and the quantum yield has an average value of 0.0065 ± 0.0004 adduct formed per photon absorbed, or 0.65 ± 0.04%.

Quantum Yield of Conversion of Furan-Side Monoadduct to Diadduct. To determine the quantum yield of diadduct formation, a "pulse–chase" experiment was performed which monitored the conversion of furan-side 8-MOP–thymidine monoadduct to dT–8-MOP–dT diadduct as a function of energy absorbed. As reported elsewhere, irradiation of a psoralen/DNA mixture with 380–400 nm light results in the formation of predominantly monoadduct (Chatterjee & Cantor, 1978). Therefore, the pulse sample was generated by irradiation of an 8-MOP/DNA solution with 397.9 nm light

Table I: Adduct Distribution in 8-MOP/DNA Irradiated at 341.5 and 397.9 nm

irradiation wavelength	base pairs/ 8-MOP bound	% of tritium recovered from HPLC: furan D_1	furan D_2	pyrone	cross-link	total tritium recovered (%)[a]
341.5	23	6	16	23	41	103
397.8	28	18	56	7	7	99

[a] Percent of total tritium injected.

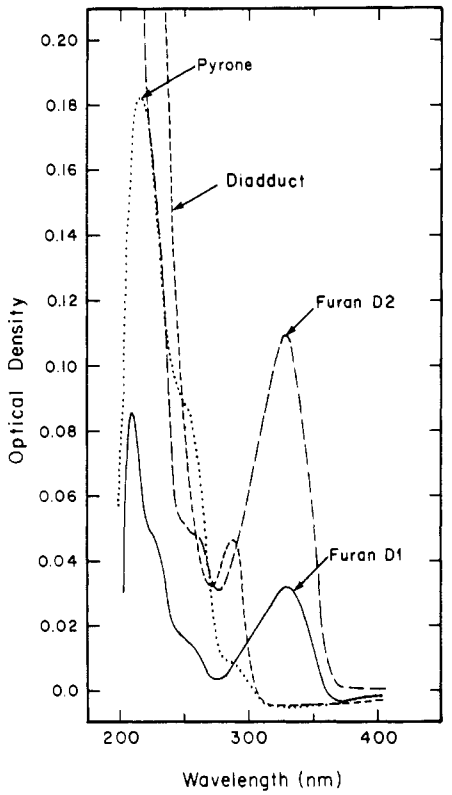

FIGURE 4: Absorption spectra of the two diastereomeric furan-side 8-MOP–dT monoadducts [D_1 (—), 1.0 μg/mL; D_2 (– – –), 2.7 μg/mL], the pyrone-side 8-MOP–dT monoadduct [(···) 2.7 μg/mL], and the dT–8-MOP–dT diadduct [(– · –) 11.5 μg/mL]. The spectra were determined in 30% methanol–70% 20 mM KH_2PO_4, pH 2.2.

followed by extraction and precipitation to remove unreacted 8-MOP from the DNA. A sample of the 397.9 nm generated 8-MOP/DNA was then enzymatically digested and analyzed by HPLC to determine the adduct distribution. The results of typical irradiations at 341.5 nm and 397.9 nm are shown in Table I. At a similar overall binding ratio, the amount of furan-side monoadduct and diadduct formed is different at the two wavelengths. While nearly half the total adduct is diadduct with 341.5 nm light, only 5–10% diadduct is formed when 397.9 nm light is used for the irradiation.

In the chase portion of the experiment, the 397.9 nm bound 8-MOP/DNA was reirradiated at 341.5 nm for several different time points. The conversion of furan-side monoadduct to diadduct was followed at each of these points by enzymatic digestion and HPLC analysis, while the number of photons absorbed was determined as described under Experimental Procedures. As shown in Figure 4, the only species present capable of absorbing an appreciable amount of 341.5 nm light was furan-side monoadduct. Since not every furan-side monoadduct was converted to diadduct, the total number of photons absorbed was multiplied by the fraction of furan-side monoadduct which was converted at light saturation (i.e., additional irradiation resulted in no additional diadduct formation). This number was used in the quantum yield calculation.

Table II: 341.5-nm Chase of 397.9 nm Generated 8-MOP/DNA

energy of 341.5-nm light absorbed (J)	base pairs/ 8-MOP bound	% of tritium recovered from HPLC: furan D_1	furan D_2	pyrone	cross-link	total tritium recovered (%)[a]
0	88	5.0	70.5	7.5	10.5	108
0.022	91	4.5	65.5	8.0	15.0	105
0.065	89	4.0	59.5	9.0	20.0	105
0.095	90	4.5	53.0	10.0	26.0	109
0.49	89	4.5	28.0	16.0	44.5	103
1.16	94	2.5	15.0	17.5	58.0	106
3.12	94	2.0	11.0	16.0	63.5	109

[a] Percent of total tritium injected.

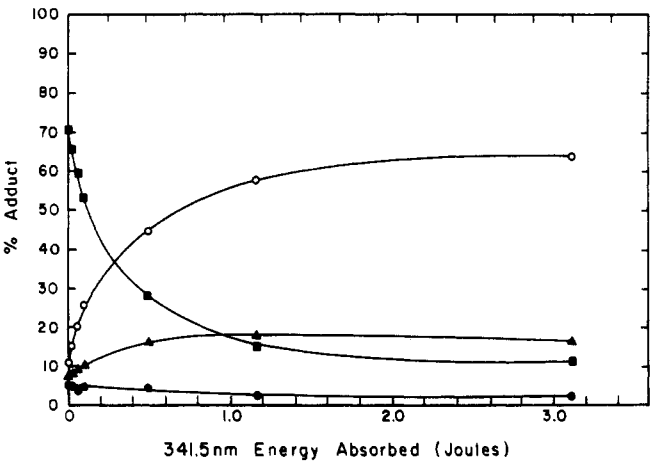

FIGURE 5: Chase irradiation of 397.9 nm generated 8-MOP/DNA with 341.5 nm light. Conversion of the two furan-side 8-MOP–dT diastereomers D_1 (●) and D_2 (■) to dT–8-MOP–dT diadduct (○) and pyrone-side 8-MOP–dT monoadduct (▲) is shown.

8-MOP can react from either the 3′ or the 5′ face of thymidine, depending on whether the 8-MOP is positioned on top of or underneath the thymine base within the binding site. Reaction within either a 5′-TpX (3′ face) or 5′-XpT (5′ face) sequence results in a pair of diastereomeric monoadducts being formed. In the case of furan-side diastereomers, resolution by HPLC is possible, and the two stereoisomers are referred to as D_1 and D_2 with respect to their chromatographic elution order. The absolute stereochemistry of the two furan-side monoadducts can be assigned by analogy with the two corresponding furan-side monoadducts formed between 4′-(hydroxymethyl)-4,5′,8-trimethylpsoralen (HMT) and thymidine. The absolute stereochemistry of these monoadducts has been determined in a previous study (Gamper et al., 1984). By comparison of the sign of the molar ellipticity of the HMT–thymidine furan-side diastereomeric monoadducts with the 8-MOP–thymidine furan-side diastereomers, D_1 corresponds to 8-MOP bound to the 5′ face of thymidine, while D_2 corresponds to 8-MOP bound to the 3′ face of thymidine. It is interesting to note that the chromatographic elution order of the HMT furan-side diastereomeric pair is the opposite of the two 8-MOP furan-side diastereomers, with the absolute stereochemistry of HMT–thymidine furan-side monoadduct D_1 being the same as the 8-MOP–thymidine furan-side monoadduct D_2. A similar pair of dT–8-MOP–dT diadduct diastereomers is also formed in the DNA; however, these are not resolved and are reported simply as diadduct. The pyrone-side monoadduct is likewise reported as a single species.

The results of these experiments are summarized in Table II and illustrated in Figure 5. Reirradiation with 341.5 nm

Table III: Comparison of Irradiation with the YAG Laser (341.5 nm) and Continuous Wave Device (320–380 nm)[a]

	energy absorbed (J)	% of tritium recovered from HPLC				total tritium recovered (%)[b]
		furan D_1	furan D_2	pyrone	cross-link	
397.9-nm irradiated 8-MOP/DNA		8	70	7	5	101
397.9-nm 8-MOP/DNA chased with 341.5 nm	7	5	10	19.5	53	103
397.9-nm 8-MOP/DNA chased with 320–380 nm	9	5	10	18	56.5	103

[a] The 8-MOP:base pair ratio was ca. 1:100. [b] Percent of total tritium injected.

light of 8-MOP/DNA adducts generated with 397.9 nm light resulted in three distinct events. First, the combined furan-side monoadduct decreased from 75.5% to 13.0%. Second, diadduct increased from 10.5% to 63.5%. Third, pyrone-side monoadduct increased from 7.5% to 16.0%. The increase in diadduct (53%) when added to that of the pyrone monoadduct (8.5%) accounts for essentially all of the observed decrease of the two furan-side monoadducts during the 341.5-nm chase.

The quantum yield of diadduct formation was determined from the linear region of the percent diadduct vs. energy absorbed plot shown in Figure 5. The quantum yield for conversion of furan monoadduct to cross-link is 2.8 ± 0.4%, which is approximately 4 times the quantum yield for initial adduct formation.

Conversion of Furan-Side Monoadduct to Pyrone-Side Monoadduct. As noted in the above section, the pyrone-side monoadduct increased 8.5% in the course of the 341.5-nm chase experiment. Since there was no free 8-MOP at the beginning of the chase, the additional pyrone-side monoadduct must have been derived from the 397.9-nm pulse sample. Possible sources of the additional pyrone-side monoadduct were (1) photoreversal of diadduct, (2) photoreversal of furan-side monoadduct followed by diffusion out of the DNA, reintercalation, and subsequent photoaddition, and (3) direct conversion or "photoisomerization" of furan-side to pyrone-side monoadduct. To investigate these three mechanisms, the following experiments were carried out.

As an initial control experiment to rule out the possibility that the increase of pyrone monoadduct resulted from the high photon density of the pulsed laser light source as opposed to the reduced photon density of the continuous wave device, an experiment was performed that compared irradiation with a pulsed laser to a broad-band source. By use of the laser and the continuous wave device described under Experimental Procedures, 397.9-nm generated 8-MOP/DNA pulse samples were reirradiated with 341.5 and 320–380 nm light, respectively. Adduct distributions of the samples were determined as before. As shown in Table III, the results were essentially the same at 341.5 and 320–380 nm, with the pyrone-side monoadduct increasing 9–10% from its value in the pulse sample.

Next, the ability of isolated nucleoside furan-side monoadduct, nucleoside pyrone-side monoadduct, and dinucleoside diadduct to photoreverse at 341.5 nm was tested. HPLC fractions of the various adducts were pooled, evaporated, and redissolved in 10 mM Tris/1 mM EDTA buffer (pH 7.5) and then irradiated individually at 341.5 nm. HPLC analysis found no photoreversal of the nucleoside pyrone-side monoadduct or dinucleoside diadduct had occurred, while the furan-side nucleoside monoadduct had undergone extensive photoreversal.

Having demonstrated that photoreversal could occur at 341.5 nm with nucleoside furan-side monoadduct, the question of in-helix furan-side monoadduct photoreversal was addressed by continued irradiation of an 8-MOP/DNA pulse sample well beyond the last time point measured in Figure 5. The irradiation was performed at 320–380 nm and also at 341.5 nm. No significant change in the binding ratio of 8-MOP to DNA base pairs was found; therefore, the 8-MOP once bound is stable and is not removed from the DNA upon irradiation with these wavelengths.

Discussion

The photo-cross-linking of native, intact DNA by 8-methoxypsoralen is a multistep reaction which involves (1) formation of a noncovalent complex between 8-MOP and DNA, resulting from intercalation of 8-MOP within the DNA helix, (2) formation of covalent monoadduct via cycloaddition between the 5,6 double bond of thymidine and the 3,4 or 4′,5′ double bond of 8-MOP, and (3) conversion of a portion of the furan-side monoadduct to diadduct in a second photochemical event. This third step can occur only with appropriately situated furan-side monoadducts which are located in cross-linkable sites. A fourth reaction also occurs in which some of the furan-side monoadduct is converted to pyrone-side monoadduct, probably via interstrand photoisomerization. This mechanism also requires the furan-side monoadduct to be in a cross-linkable site.

The reactions leading to monoaddition and diadduct formation between 8-MOP and thymidine and the possible photoisomerization of furan-side monoadduct to pyrone-side monoadduct can be expressed as follows:

$$P + S \rightleftarrows PS \quad \text{intercalation} \quad (1)$$

$$PS + h\nu \rightarrow MA_f + MA_p \quad \text{monoaddition} \quad (2)$$

$$MA_f + h\nu \rightarrow XL \quad \text{diadduct formation} \quad (3)$$

$$MA_f + h\nu \rightarrow MA_p \quad \text{[photoisomerization]} \quad (4)$$

Here P is free 8-MOP in solution, S is an 8-MOP binding site in the DNA (defined here as a base pair), PS is the noncovalent intercalation complex of 8-MOP in a binding site, MA_f is covalent monoadduct between the furan side of 8-MOP and thymidine, MA_p is covalent monoadduct between the pyrone side of 8-MOP and thymidine, and XL is diadduct where both sides of 8-MOP are bound to thymidines on opposing strands of the helix. During the irradiation, other processes occur including dimerization and photobreakdown of free 8-MOP in solution. These reactions have not been considered in this report. What has been investigated is (1) the quantum yield of initial adduct formation between 8-MOP and DNA, (2) the quantum yield of conversion of monoadduct to diadduct (reaction 3), and (3) the mechanism of conversion of furan-side monoadduct to pyrone-side monoadduct (reaction 4).

Quantum Yield of Initial Adduct Formation. The quantum yield for initial adduct formation of 8-MOP to DNA was determined to be 0.65 ± 0.04% by using monochromatic 341.5-nm light. The calculation was based on the assumption that the amount of intercalated 8-MOP did not change significantly at the time points the measurements were taken. This assumption is justified for the following two reasons. First, only 11% of the total 8-MOP had undergone photoaddition at the last time point used for the quantum yield calculation. Second, 8-MOP photoreacts with DNA much faster than it undergoes photochemical breakdown when free in

solution (Isaacs et al., 1982). According to the equilibrium expression, removal of 8-MOP by either photoaddition or photobreakdown would lower the absolute number of 8-MOP molecules intercalated within the helix; however, this effect is quite small when only 11% of the 8-MOP has undergone photoaddition to the DNA. The slightly negative slope of the quantum yield plot in Figure 4 could reflect a heterogeneity in binding sites within the DNA, with a small number of favored sites having a slightly higher quantum yield.

In a previous report from this laboratory (Isaacs et al., 1982), the quantum yield for reaction 2 was reported to be 1.3% by using a broad-band light source which delivered wavelengths between 320 and 380 nm. The difference in the two numbers is in part due to the differences in irradiation conditions and also due to an improved method for determining the number of photons absorbed.

The photoreaction of 8-MOP with calf thymus DNA at 365 nm has also been addressed in three other papers. In one study, a quantum yield of 4.6×10^{-3} which was not corrected for the absorbance of nonintercalated 8-MOP was reported (Rhodighiero et al., 1970). By use of their 8-MOP and DNA concentrations and a K_D of 1.8×10^{-3}, such a correction would give a quantum yield of approximately 9.2×10^{-3}. This is close to the value we report, and the difference may be due to the differences in irradiation conditions. In another report, an overall quantum yield of 1.4×10^{-3} was determined for the reaction (Ou et al., 1978). Again, this can be corrected for the absorbance of nonintercalated 8-MOP to give a quantum yield of approximately 5×10^{-3}. The difference in the magnitude of the two correction factors is due to a difference in the 8-MOP:DNA base pair ratio used in the two experiments. This overall quantum yield was calculated after 4 h of irradiation, and an initial quantum yield would be higher and perhaps closer to our value. Finally, rates of the various photoreactions of 8-MOP with DNA have been calculated from a mathematical model for both monoadduct and diadduct formation (Dall'Acqua et al., 1979). However, this model does not directly deal with the quantum yield of initial adduct formation.

Quantum Yield of Conversion of Furan-Side Monoadduct to Diadduct. To determine the quantum yield of reaction 3, a 397.9-nm 8-MOP/DNA stock was prepared that contained predominantly furan-side monoadduct which was subsequently converted to diadduct with 341.5 nm light. The efficiency of the conversion was measured by direct analytical methods in which each of the known adducts was quantified following various doses of 341.5 nm light. Several interesting results were found.

The first important finding was that the adduct distribution in DNA samples differed depending on whether 341.5 or 397.9 nm light was used as shown in Table I. At 341.5 nm, the primary product is diadduct while at 397.9 nm it is furan-side monoadduct, although a small but definite number of diadducts were formed at 397.9 nm.

In the chase portion of the experiment, the quantum yield of the conversion of furan-side monoadduct to diadduct was determined to be $2.8 \pm 0.4\%$. This value is 4 times higher than the quantum yield for initial adduct formation between 8-MOP and DNA. This higher efficiency for conversion of monoadduct to diadduct can be partially explained by considering the geometry of the monoadduct compared to a nonbound 8-methoxypsoralen intercalated within a potential binding site (Peckler et al., 1982). Psoralens are able to cross-link nucleic acid as a result of the overlap of the furan and pyrone bonds of the psoralen with the 5,6 double bond of thymidine on adjacent strands of the helix. The relatively low efficiency for the conversion of intercalated 8-MOP to monoadduct argues that the probability of having the appropriate photoexcited state along with the correct geometrical alignment for photocycloaddition is quite low. While an 8-MOP intercalated within a binding site will sometimes be positioned correctly for initial monoaddition, the monoadduct may be in a preferred position for the second photocycloaddition to occur. This could be due to the fact that intercalated 8-MOP is in dynamic equilibrium with nonbound 8-MOP outside the helix, while the position of the monoadduct within the cross-linking site is constrained by the covalent bond at the furan side of the molecule (Peckler et al., 1982). The bond overlap between the monoadduct and second thymidine might be enhanced compared to nonbound 8-MOP within a binding site. A second possibility is that the two reactions proceed by different photochemical mechanisms with a different efficiency for each conversion. A complete explanation of the observation will require further study.

Only the furan-side monoadduct was converted to diadduct in the chase part of the experiment. This result confirms a previous report that pyrone-side monoadduct is unable to undergo further reaction when irradiated with 320–380 nm light (Kanne et al., 1982b). Pyrone-side monoadduct actually increased in the course of the chase, typically doubling its value to over 15% of the total adduct following the chase.

Photoisomerization of Furan-Side Monoadduct to Pyrone-Side Monoadduct. An increase in pyrone-side monoadduct during the 341.5-nm chase of the 397.9 nm generated 8-MOP/DNA stock was repeatedly observed in a number of different experiments. A series of experiments were carried out to investigate the mechanism of this reaction. After it was shown that the increase in pyrone-side monoadduct occurred with both monochromatic light from the pulsed laser (341.5 nm) and broad-band light from the continuous wave device (320–380 nm), the ability of the isolated furan-side and pyrone-side monoadducts and the dT–8-MOP–dT diadduct to undergo photoreversal at 341.5 nm was investigated. Inspection of the absorption spectra in Figure 4 shows the pyrone-side monoadduct and the diadduct have no appreciable absorbance at 341.5 nm and, as expected, were found to be stable to photoreversal at this wavelength. A mechanism whereby furan-side monoadduct is converted to cross-link followed by photoreversal to generate pyrone-side monoadduct is therefore ruled out.

In contrast, the furan-side monoadduct exhibits a strong absorption at 341.5 nm and was found to undergo photoreversal at this wavelength. A plausible mechanism for conversion of furan-side monoadduct to pyrone-side monoadduct suggested by this result is the following. Absorption of 341.5 nm light by furan-side monoadducts in non-cross-linkable sites causes in-helix photoreversal to occur. The nonbound 8-MOP formed in this process diffuses out of the helix, intercalates in a new binding site, and forms a new monoadduct. A certain portion of these new monoadducts would be pyrone side. Simultaneously, some of the new furan-side monoadducts in cross-linkable sites would be converted to diadduct. This mechanism predicts that, given enough light, all the furan-side monoadduct would disappear from the DNA having been converted either to pyrone side or to diadduct or photodestroyed during the unbound phase as free 8-MOP in solution. Since initially almost all furan-side monoadduct is present, and since photodestruction of unbound 8-MOP does occur, the total adduct level on the DNA would be predicted to decrease with prolonged irradiation. Neither of these two predictions was

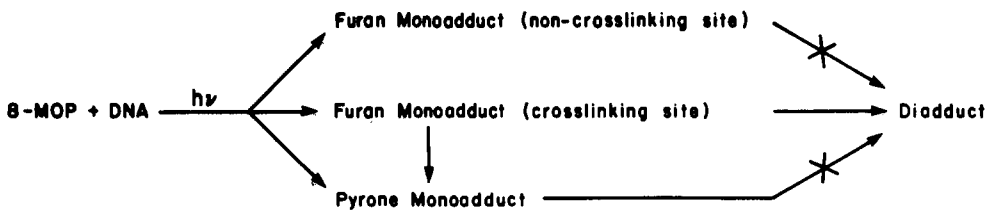

FIGURE 6: Proposed mechanism for the conversion of furan-side monoadduct to pyrone-side monoadduct and diadduct.

Table IV: Nearest-Neighbor Frequencies in Calf Thymus DNA[a] of Dinucleotides Containing Thymidine

	T-A	A-T	T-C	C-T	T-G	G-T	T-T
% nearest-neighbor frequency in DNA	6.1	7.6	6.9	6.5	7.6	6.0	8.4
% frequency of reactive sites[b]	10.6	13.2	12.0	11.3	13.2	10.4	29.2

[a] Dinucleotides are listed from the 5′ end to the 3′ end. [b] Percent frequency of reactive sites = (% nearest-neighbor frequency × number of thymidines/dinucleotide)/(Σ% nearest-neighbor frequency × number of thymidines/dinucleotide) × 100.

observed. Irradiation well beyond the time points shown in Figure 5 showed no further decrease in furan-side monoadduct (Table III) and no significant change in the level of binding of 8-MOP per DNA base pair (data not shown). We therefore conclude that photoreversal, diffusion out of the helix, and new monoadduct formation are not occurring and cannot account for the observed increase in pyrone-side monoadduct.

An alternative explanation, which we propose to be operative here, is that furan-side monoadduct undergoes in-helix photoreversal but does not diffuse out of the helix. Instead, one of two events occurs. In the first case, the furan-side monoadduct is simply re-formed with no net change in either type or number of adducts present in the DNA. This process occurs primarily with furan-side monoadducts that are located in non-cross-linkable sites. In the second case, with furan-side monoadducts located in cross-linkable sites, the excited furan monoadduct photoisomerizes, re-forming at the pyrone end of the 8-MOP with the available thymidine on the opposite strand, thereby forming pyrone-side monoadduct. This mechanism is consistent with the observed experimental result that no net change in total adduct bound to the DNA occurs. Thus, absorption of 341.5 nm light by furan-side monoadduct in a cross-linkable site can lead to cross-link or to pyrone-side monoadduct via photoisomerization. With furan-side monoadducts in non-cross-linkable sites, no conversion can occur, and the adduct simply re-forms following excitation. In both cases, the excitation/bond-breaking/bond-making processes are clearly faster than diffusion of the transient noncovalently bound 8-MOP out of the DNA helix. The proposed conversions which occur are summarized in Figure 6.

Preferential Monoaddition at 5′-TpA Cross-Linkable Sites in the DNA. Inspection of Table II shows that at low binding levels the two diastereomeric furan-side 8-MOP–dT monoadducts D_1 and D_2 were formed in a 1:14 ratio. This indicates a large preference for reaction on the 3′ face of the thymidine. Assuming our model for photoisomerization is correct, we observe that 72% of the 8-MOP bound to the DNA is in a cross-linkable site. Furthermore, if the D_1:D_2 ratio of 1:14 is applied to the cross-link formed at 397.9 nm, 69% of the 8-MOP bound is in a 5′-TpA site. One notes from Table IV that roughly 10.6% of the reactive sites are 5′-TpA (Fasman, 1976). Thus, the preferential binding of 8-MOP to calf thymus DNA is to 5′-TpA cross-linkable sites in the DNA.

There are three possible explanations of this preference: (1) the 8-MOP intercalates preferentially into a 5′-TpA site and photoreacts equally well in all sites; (2) the 8-MOP intercalates equally well into all sites and photoreacts preferentially with the 5′-TpA sites; (3) the 8-MOP prefers both intercalation into and photoreaction with a 5′-TpA site. Molecules such as acridine orange and ethidium ion which, like psoralens, intercalate into DNA show a sequence-binding preference for 5′-pyrimidine–purine sites in dinucleotides and short oligonucleotides (Sobell et al., 1982). This observation may not apply to intercalation into a high molecular weight double-stranded DNA. However, if this observation is valid for intact DNA, it would support the idea that the preferential binding of 8-MOP to a 5′-TpA site in the DNA is due to favorable intercalation into this site. However, it would still be unclear as to whether the photoreaction of 8-MOP in a 5′-TpA site were preferential as well. One possible interpretation of the data to date suggests that all 5′-TpA sites react 22 times faster than the remaining thymidine sites which are equivalent to each other. To determine the explanation for the observed preference in binding would require further experiments beyond the scope of this report.

Conclusion

We have studied the photochemical reaction of 8-MOP with double-stranded calf thymus DNA. Our results show that (1) the quantum yield for conversion of furan-side monoadduct to diadduct is approximately 4 times greater than the quantum yield for initial photoaddition of 8-MOP to DNA (2.8 ± 0.4% vs. 0.65 ± 0.04%), (2) furan-side monoadduct is converted not only to diadduct but also to pyrone-side monoadduct, possibly via photoisomerization, and (3) at low levels of 8-MOP covalently bound to DNA, 8-MOP exhibits a preference for monoaddition to 5′-TpA cross-linkable sites. Irradiation at 397.9 nm to a binding ratio of approximately 100 base pairs per 8-MOP results in the formation of photoadducts of which less than 10% are diadduct. However, nearly 70% of these adducts are in 5′-TpA cross-linkable sites. It is therefore possible to bind 8-MOP to double-stranded DNA such that diadduct formation is highly favored.

Acknowledgments

We thank Professor Richard Mathies for the use of the Nd:YAG laser and Mark Trulson, Anne Myers, and Dr. Don Friedrich for their assistance in using the laser. We also thank Dr. George Cimino for his assistance with actinometry and for many helpful discussions and ideas.

Registry No. **1**, 298-81-7; **2**, 80603-65-2; **2′**, 80656-97-9; **3**, 80603-69-6; **4**, 83380-32-9; 5′-TpdA, 19192-40-6; thymidine, 50-89-5.

References

Chatterjee, P. K., & Cantor, C. R. (1978) *Nucleic Acids Res. 5*, 3619–3633.

Dall'Acqua, F., Magno, S. M., Zambon, F., & Rhodighiero, G. (1979) *Photochem. Photobiol. 29*, 489–495.

Fasman, G. D., Ed. (1976) *CRC Handbook of Biochemistry and Molecular Biology*, 3rd ed., Vol. II, p 317, CRC Press, Cleveland, OH.

Gamper, H., Piette, J., & Hearst, J. E. (1984) *Photochem. Photobiol. 40*, 29-34.
Isaacs, S. T., Shen, C. J., Hearst, J. E., & Rapoport, H. (1977) *Biochemistry 16*, 1058-1064.
Isaacs, S. T., Chun, C., Hyde, J. E., Rapoport, H., & Hearst, J. E. (1982) in *Trends in Photobiology* (Helene, C., et al., Eds.) pp 279-294, Plenum Publishing Corp., New York.
Kanne, D., Straub, K., Rapoport, H., & Hearst, J. E. (1982a) *Biochemistry 21*, 861-871.
Kanne, D., Straub, K., Hearst, J. E., & Rapoport, H. (1982b) *J. Am. Chem. Soc. 104*, 6754-6764.
Kanne, D., Rapoport, H., & Hearst, J. E. (1984) *J. Med. Chem. 27*, 531-534.
Ou, C., Tsai, C., Tapley, K. J., & Song, P. S. (1978) *Biochemistry 17*, 1047-1053.
Peckler, S., Graves, B., Kanne, D., Rapoport, H., Hearst, J. E., & Kim, S.-H. (1982) *J. Mol. Biol. 162*, 157-172.
Rhodighiero, G., Musajo, L., Dall'Acqua, F., Marciani, S., Caporale, G., & Ciavatta, L. (1970) *Biochim. Biophys. Acta 217*, 40-49.
Sobell, H. M., Sakore, T. D., Jain, S. C., Banerjee, K. K., Bhandary, K. K., Reddy, B. S., & Lozansky, E. D. (1982) *Cold Spring Harbor Symp. Quant. Biol. 47*, 293-314.
Song, P. S., & Tapley, J. K. (1979) *Photochem. Photobiol. 29*, 1177-1197.
Straub, K., Kanne, D., Hearst, J. E., & Rapoport, H. (1981) *J. Am. Chem. Soc. 103*, 2347-2355.
Thompson, J. F., & Hearst, J. E. (1983a) *Cell (Cambridge, Mass.) 32*, 1355-1365.
Thompson, J. F., & Hearst, J. E. (1983b) *Cell (Cambridge, Mass.) 33*, 19-24.
Weissberger, A., Ed. (1956) *Technique of Organic Chemistry*, Vol. II, p 257, Wiley-Interscience, New York.

Photochemical Demonstration of Stacked C·C$^+$ Base Pairs in a Novel DNA Secondary Structure†

Daniel M. Brown,‡ Donald M. Gray, and Michael H. Patrick*
Program in Molecular Biology, The University of Texas at Dallas, Richardson, Texas 75083-0688
Robert L. Ratliff
Genetics Group, Life Sciences Division, Los Alamos National Laboratory, Los Alamos, New Mexico 87545
Received May 29, 1984

ABSTRACT: The secondary structure of the alternating polydeoxynucleotide sequence poly[d(C-T)] was studied as a function of pH by ultraviolet absorbance and circular dichroism spectroscopy and by the analysis of UV-induced photoproducts. As the pH was lowered, poly[d(C-T)] underwent a conformational transition that was characterized by changes in the long-wavelength region (280–320 nm) of the CD spectrum. These changes have previously been interpreted as evidence for the formation of a core of stacked, protonated C·C$^+$ base pairs in a double-helical complex of poly[d(C-T)], with the thymidyl residues being looped out into the solvent [Gray, D. M., Vaughan, M., Ratliff, R. L., & Hayes, F. N. (1980) *Nucleic Acids Res. 8*, 3695-3707]. In the present work, poly[d(C-T)] was labeled with [U-^{14}C]cytosine and [*methyl*-^{3}H]thymine and irradiated at pH values both above and below the conformational transition point (monitored by CD spectroscopy). The distribution of radioactivity in uracil<>uracil dimers, uracil<>thymine dimers (the deamination products of cytosine<>cytosine and cytosine<>thymine dimers, respectively), and thymine-<>thymine dimers was then determined. As the pH was decreased, we found an increase in the yield of uracil<>uracil dimers and a decrease in the yield of uracil<>thymine dimers, which occurred concomitantly with the change in the CD spectrum. These changes were interpreted as evidence that a stacked C·C$^+$ base-paired structure was indeed formed by alternate cytosine bases in poly[d(C-T)] at acid pH, with the thymidyl residues being individually looped out of the structure. The dose-dependent kinetics of photoproduct formation and a loss of the long-wavelength CD band of the irradiated poly[d(C-T)] self-complex indicated that the structure was destabilized during irradiation, due to dimerization of the looped-out thymines. Taken together with the previous study showing that other cytosine-containing sequences may exist in a similar conformation (Gray et al., 1980), these results show that a new range of conformations is accessible to DNA.

Synthetic DNA polymers of various sequences have been shown to undergo acid-induced structural rearrangements as indicated by changes in their CD[1] spectra (Gray et al., 1978, 1980; Thiele et al., 1978a,b; Marck et al., 1978). Upon addition of acid to solutions of synthetic cytosine-containing DNA polymers, increased positive CD values are observed in the long-wavelength region (280–320 nm) of the spectrum, where the absorption is dominated by cytosine. For poly[d-

† This work was performed by D.M.B. in partial fulfillment of the requirements for the Ph.D. degree in the Molecular Biology Program, The University of Texas at Dallas. We are grateful for support by NIH Research Grant GM 19060 from the National Institute of General Medical Sciences and by Grant AT-503 from the Robert A. Welch Foundation. Work at the Los Alamos National Laboratory was supported by the U.S. Department of Energy. A preliminary report of this work was presented at the 27th Annual Biophysical Society Meeting (Brown et al., 1983).
‡ Present address: School of Physics, Georgia Institute of Technology, Atlanta, GA 30332.

[1] Abbreviations: CD, circular dichroism; C<>C, C<>T, T<>T, U<>U, and U<>T, pyrimidine dimers (cyclobutyl dipyrimidines) of cytosine–cytosine, cytosine–thymine, thymine–thymine, uracil–uracil, and uracil–thymine, respectively; Tris-HCl, tris(hydroxymethyl)aminomethane hydrochloride.

0006-2960/85/0424-1676$01.50/0